JOURNAL OF MATERIALS SCIENCE 30 (1995) 5438–5448

Pilot-scale casting of single-crystal copper wires by the Ohno continuous casting process

H. SODA, A. McLEAN, Z. WANG
Department of Metallurgy and Materials Science, University of Toronto, Toronto, Ontario, Canada

G. MOTOYASU*
Department of Metallurgical Engineering, Chiba Institute of Technology, Narashino-shi, Chiba-ken, Japan

Single-crystal copper wires, 4 mm in diameter, have been produced using the horizontal Ohno continuous casting (OCC) process and a casting regime for the production of single crystals has been established. It was found that at lower casting speeds ($< 50\ mm\ min^{-1}$), single-crystal wires with no visible substructures were produced. However, at casting speeds above $50\ mm\ min^{-1}$, the wire contained unidirectional subtexture and occasional stray crystals. The orientation of crystals parallel to the casting direction tended to be $\langle 0\,0\,1 \rangle$ at higher casting speeds ($\sim 120\ mm\ min^{-1}$); at lower casting speeds, the orientation appeared to be random. It was also found that the solidifying wire recrystallized as it emerged from the mould if local strains were inflicted upon the cast surface by mould–strand friction.

1. Introduction

Bulk industrial single crystals, such as silicon crystals, are mostly grown using the Czochralski method. However, although this method produces large, high-quality single crystals and is an indispensable technique for the electronic industry, it is not suited for the production of net-shape single-crystal wires of substantial length. Other crystal-growth methods, such as the Bridgman–Stockbarger technique, offer good means for small- and large-scale production of single crystals of metallic and non-metallic materials. Copper single crystals have been grown mostly by the Bridgman–Stockbarger technique [1], in which materials are contained in a mould (crucible) which travels through a temperature gradient in the furnace, or alternatively the furnace moves along the mould [2]. In this technique, the length of crystal is limited by the size of the mould. On the other hand, in the Ohno continuous casting (OCC) process, the mould remains stationary within the heated zone from which a solidified crystal is withdrawn continuously as in the case of the conventional cooled-mould continuous casting system, thereby making it possible to produce metallic single crystals of small diameter but unlimited length [3]. This is the principal advantage of the OCC process. The process is used commercially to produce single-crystal or unidirectionally solidified copper wires and rods for specific applications, such as audio and video cables. However, despite successful commercial implementation, only a few technical details have been made available regarding the operational aspects of the process and characterization of the cast copper products [4, 5]. Thus, this paper describes some work that has been performed on the production and characterization of copper single-crystal wires, 4 mm in diameter.

2. The casting process

2.1. Melting and casting equipment

Fig. 1 shows a schematic illustration of the OCC equipment which consists of a melting furnace, a cylindrical graphite displacer block for molten metal level control, a graphite mould, a cooling device, and pinch rolls for withdrawal of the cast product. The graphite crucible in the furnace is capable of holding about 16 kg of copper. The heating element for the furnace was Kanthal wire, 5.5 mm in diameter. The maximum current was 48 A. The furnace was equipped with a wire feeding device to provide melt stock for the crucible and to maintain the molten metal at a constant level.

The graphite mould, 50 mm long and 25 mm diameter, is heated with Kanthal wire, 3.5 mm diameter with a 1.3 Ω resistance. The maximum current was 35 A. The mould has a cylindrical channel, 25 mm long and 4 mm diameter, which determines the diameter of the cast wires. The remainder of the channel

* Visiting scientist at the University of Toronto.

0022–2461

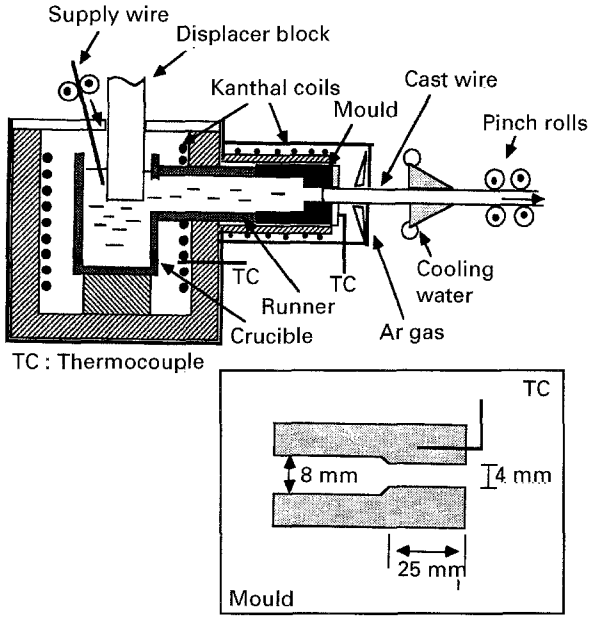

Figure 1 Schematic illustration of the OCC equipment.

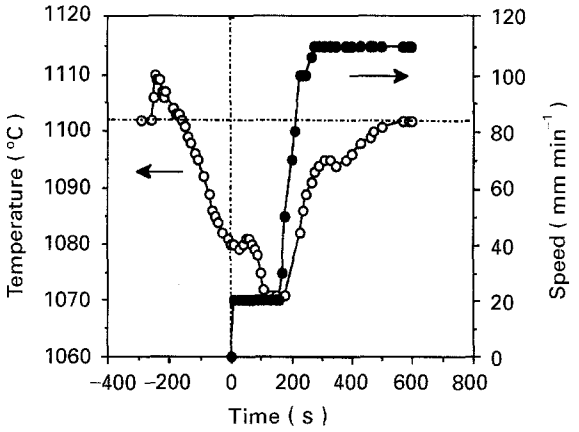

Figure 2 The timing of commencement of casting and subsequent increase in casting speed in relation to changes in the control temperature.

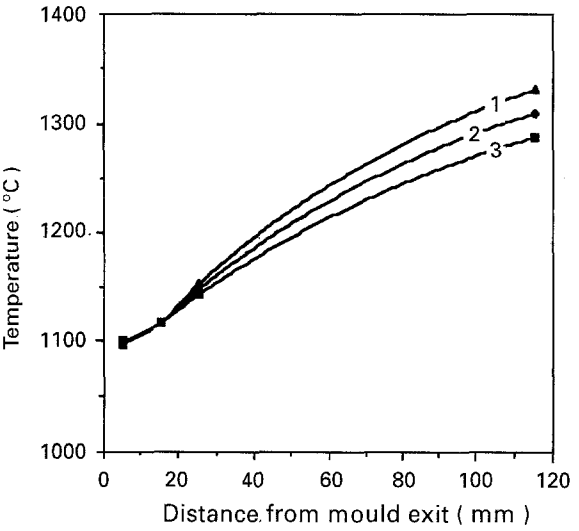

Figure 3 Temperature distribution within the mould and runner during steady-state casting at casting speeds of (1) 20, (2) 40 and (3) 60 mm min^{-1}.

diameter was 8 mm, as shown in Fig. 1. The control thermocouple was placed at 15 mm from the mould exit in the mid-thickness of the mould wall and was controlled within ± 1 °C of the target temperature. The temperature at this location is termed the "control temperature". The cylindrical cooling device has eight 0.8 mm water outlet orifices. The amount of cooling water was approximately 800 ml min^{-1}. The cooling device can be moved between 33 and 93 mm away from the mould exit; however, in this work, this distance was kept at 33 mm.

2.2. Start-up procedure

Commercially available oxygen-free copper was melted under a high-purity argon atmosphere. The furnace temperature was kept at 1160 °C which maintains the melt temperature at 1154 °C, which is about 70 °C above the melting point of copper. Before introducing molten metal to the mould, the control temperature was set at 1104 °C in order to assist the flow of the metal, and a stainless steel dummy bar was located at the mould exit. When the temperature attained the set value, the molten metal was fed into the mould by lowering the displacer block into the crucible and bringing the metal level above the metal intake connected to the mould. As soon as the molten metal filled the mould, the water was turned on and the control temperature setting was lowered to 1082 °C to aid solidification within the mould, in order to avoid breakout at start-up. When the temperature dropped to 1084 °C, casting commenced with a speed of 20 mm min^{-1}. As soon as the control temperature dropped to 1082 °C, the casting speed was increased gradually to about 100 mm min^{-1} in order to raise the mould temperature and to bring the solid–liquid interface closer to the mould exit. At the same time, the control temperature setting was also reset to the target value. The control temperature was not permitted to fall below 1077 °C in order to avoid breaking of the cast wires due to excess friction between solid wire and the mould wall. Fig. 2 shows a typical example of the commencement of casting and subsequent increase of casting speed in relation to the control temperature reading during start-up. Steady-state conditions were achieved after about 500 s or after about 60 cm wire had been cast. Fig. 3 shows an example of the temperature profile within the mould and runner during steady-state casting conditions. The casting speed was varied between 20 and 60 mm min^{-1}, and the control temperature was kept constant at 1117 °C. In previous work [6], the temperature gradient, G_L, in the liquid ahead of the solidification front for tin and Al–4% Cu alloy was correlated with ΔT (the difference between the control temperature and the solidification temperature of metal being cast). From this correlation, the value of G_L for copper was estimated to be about 9–10 °C mm^{-1}. Fig. 4 is a photograph showing copper wire, 4 mm in diameter, leaving the cooling device. The cast wires were examined using optical microscopy, SEM, electron channelling pattern analysis and the Läue back-reflection X-ray method.

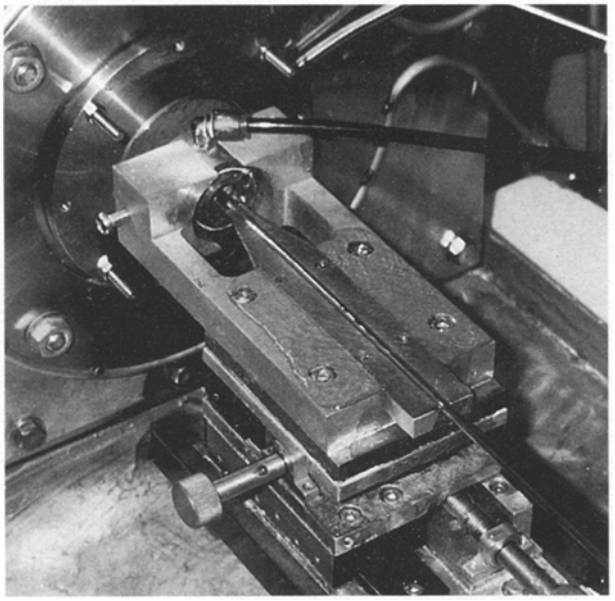

Figure 4 Casting of copper wire of 4 mm diameter.

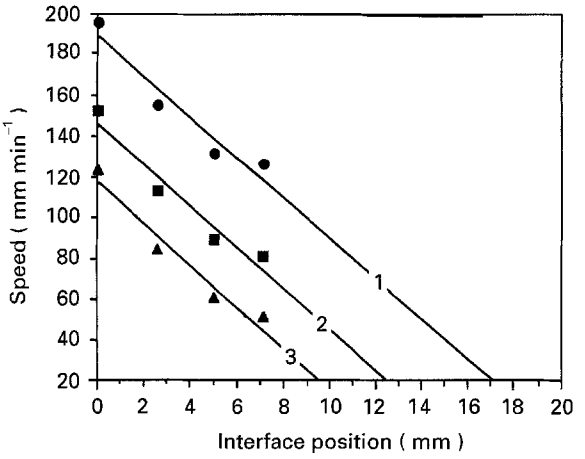

Figure 6 The solid–liquid interface location in relation to the casting speed. The location is expressed as distance from the mould exit. Control temperature: (1) 1083 °C, (2) 1117 °C, (3) 1140 °C.

3. Results and discussion

3.1. The solid–liquid interface position

In order to have better control of the casting process, it is desirable to know the solid–liquid interface position in relation to the casting speed and the controlled mould temperature. This was determined in the following manner. Shallow grooves were made in the wall of each mould extending 2.6, 5.0 and 7.1 mm from the mould exit, and casting conditions were adjusted by changing the casting speed and the control temperature. If the solid–liquid interface reaches the groove end, a projection will appear or disappear on the cast surface of the wire according to the casting speed and the control temperature. In this way, the casting conditions for which the solid–liquid interface is at 2.6, 5.0 and 7.1 mm positions, can be determined. Fig. 5 shows the solid–liquid interface locations in terms of the casting speed and the control temperature. Breakout occurred at a casting speed of 150 mm min^{-1} and a control temperature of 1119 °C, denoted by X in Fig. 5. Because all three lines in this figure are approximately parallel to each other, a dotted line passing through the point X and parallel to these three lines is considered to represent the solid–liquid interface position at the mould exit. From Fig. 5, the solid–liquid interface location with respect to the mould exit can be expressed in relation to the casting speed for different control temperatures, as shown in Fig. 6. For example, with a control temperature of 1117 °C the solidification front moves from approximately 12.5 mm to 2.5 mm from the mould exit as the casting speed increases from 20 mm min^{-1} to 120 mm min^{-1}.

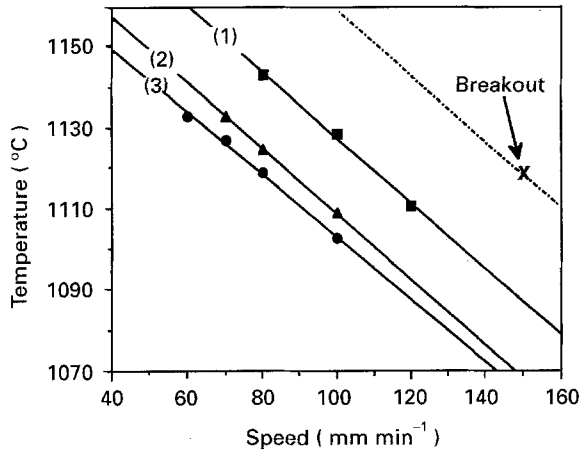

Figure 5 The solid–liquid interface position in relation to changes in the casting speed and the control temperature. The mould–cooler distance was 33 mm. Solid–liquid interface position: (1) 2.6 mm, (2) 5.0 mm, (3) 7.1 mm.

3.2. Factors affecting the cast structure

3.2.1. Mould-surface condition

Unlike the casting of tin wires of 2 mm diameter by the OCC process, in which the solid–liquid interface existed outside the mould [7], for casting of copper wires of 4 mm diameter, the solid–liquid interface clearly exists within the mould. Thus the mould condition will significantly influence the cast surface of the wires and also the cast structure. Recrystallization may occur if local plastic strain caused by friction is too large. For these reasons, the mould must be made with a smooth surface and good dimensional accuracy.

In order to observe the effect of the mould surface condition on cast structure, a groove was made on the top surface of the mould so that the top surface of the wire did not touch the mould surface during solidification. The remainder of the mould produced streaks on the copper wire due to interaction with the mould surface. Fig. 7 shows a cast sample after acid etching which clearly reveals that the equiaxed grains exist only on the side of the wire which has streaks. In fact, observations of structure at high magnification showed a typical recrystallized grain structure. This confirms that recrystallization is due to plastic deformation inflicted upon the wire surface by friction. Thus, it is essential to use a mould with a high-quality surface and dimensional accuracy in order to produce single-crystal products.

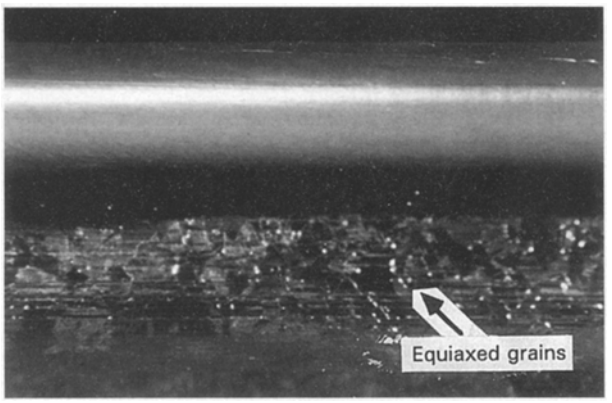

Figure 7 The cast sample showing the recrystallized equiaxed grains on the streaked side only.

3.2.2. Casting speed

Macroscopic examination of the cast surface of the specimens revealed that casting speed exerted a significant effect on the structure. A 10 cm long cast specimen was etched with a nitric acid solution to reveal surface grain structures. Fig. 8 shows examples of the surface structure of wires obtained with different casting speeds. At casting speeds of 20 and 40 mm min^{-1}, no visible surface textures were observed. This indicates that the cast wire is most likely a single crystal, whereas at casting speeds above 60 mm min^{-1}, the cast surface clearly revealed unidirectional textures which became clearer as the casting speed increased. The wire produced at a casting speed of 50 mm min^{-1} exhibited only a weak streak on one side of the rod surface. Also, there was a tendency to form stray grains at faster casting speeds. Fig. 9 is an optical micrograph showing an example of a stray grain. It is clearly visible at the edge of the cross-section.

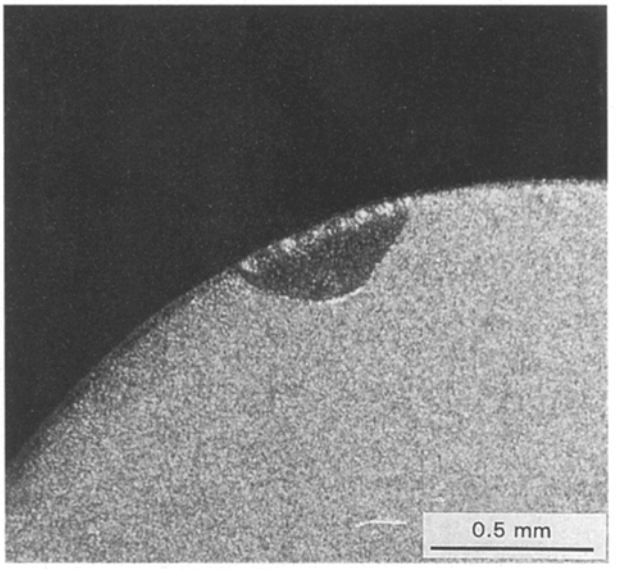

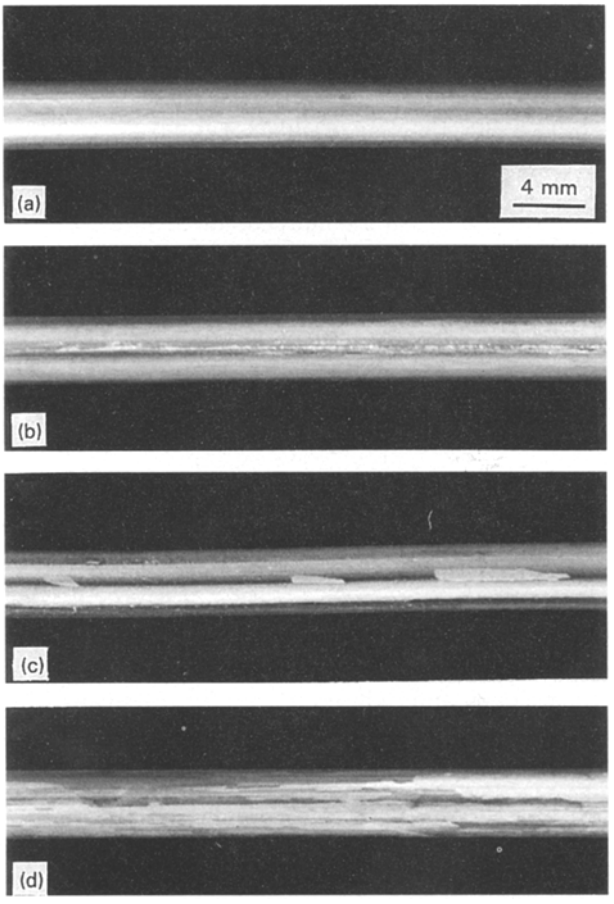

Figure 8 Cast surface structure of the wire specimens after etching with a nitric acid solution. Casting speed: (a) 40, (b) 50, (c) 60, and (d) 120 mm min^{-1}. The control temperature was 1117 °C and the mould–cooler distance was 33 mm.

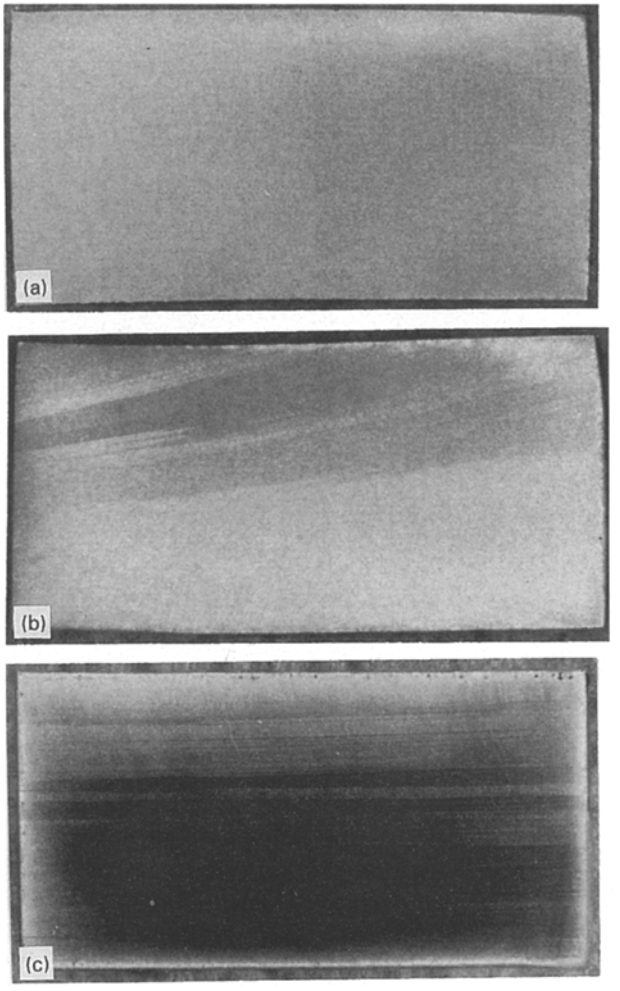

Figure 10 Change in cast structure of the wire with an increase in casting speed: (a) 20, (b) 50, and (c) 120 mm min^{-1}.

Fig. 10 shows the cast structure observed on the longitudinal cross-section of the wires. As expected from the observations of surface texture, at lower casting speeds the cross-section did not reveal any linear texture. However, when the casting speed exceeded 50 mm min^{-1}, the longitudinal sections exhibited unidirectional linear textures. These aspects correspond well with the results of surface texture observations. The transverse cross-sections of the wires were also examined using scanning electron microscopy. Fig. 11 shows micrographs of the electron channelling contrast (ECC). At the casting speeds of 20 and 40 mm min^{-1}, the specimen did not exhibit any grains; at a casting speed of 50 mm min^{-1}, grains

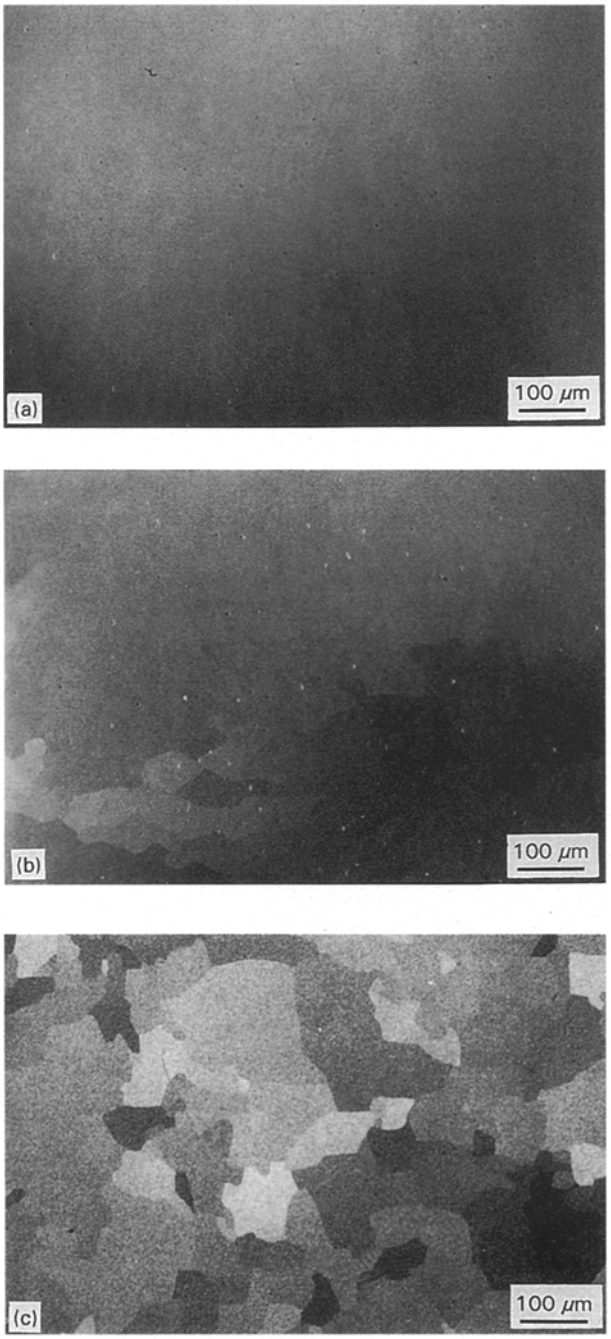

Figure 11 Micrographs of electron channelling contrast (ECC) showing changes in the cast structure of transverse cross-section of the wire with an increase in casting speed: (a) 40, (b) 50, and (c) 120 mm min^{-1}.

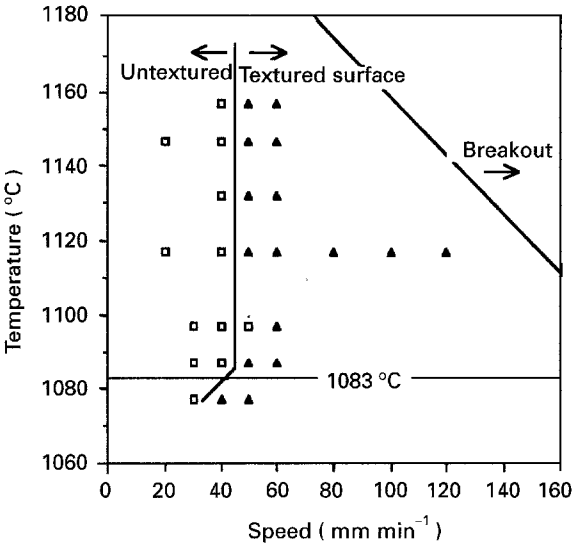

Figure 12 Casting regime diagram for wires with no visual surface texture. (□) Untextured, (▲) textured.

were partly visible and became clearly observable at higher casting speeds. These results of ECC observations further reconfirmed the results of visual surface texture observations. Thus, for a rapid visual assessment of cast products, wire produced under different casting conditions was examined immediately after etching and classified as either untextured or textured. The results shown in Fig. 12 reveal that with casting speeds under 50 mm min^{-1}, no visual textures were formed. Above 50 mm min^{-1}, clear unidirectional texture existed regardless of the control temperatures within the range examined. Fig. 12 provides a general reference point for determining the casting conditions within which the cast products will have high probability of being single crystals. From these surface-texture observations, no distinction was made between stray grains and unidirectional texture observed on the cast surface of the wires. Thus the effect of raising the controlled mould temperature on elimination of stray crystals is unknown. However, it is noted that a high temperature gradient and low growth speed can eliminate these stray crystals [8].

The probability of success in producing single crystals is influenced not only by the growth speed and temperature gradient but also by impurities [9]. Under favourable conditions, stray crystals can grow from the heterogeneous nuclei that exist in the melt. Experimental results in growing single crystals of tin, zinc and bismuth by Yamamoto and Watanabe [10, 11] showed that the probability of success was reduced linearly with an increase in the growth rate of the specimen and reduced further for specimens with a large impurity level.

3.3. Growth orientations

It is possible to obtain information about the orientation of the grains by observing etch pits. They reveal specific shapes according to the crystal plane exposed to the surface. For copper which has a face-centred cubic lattice, the etch pits on a {1 1 1} plane

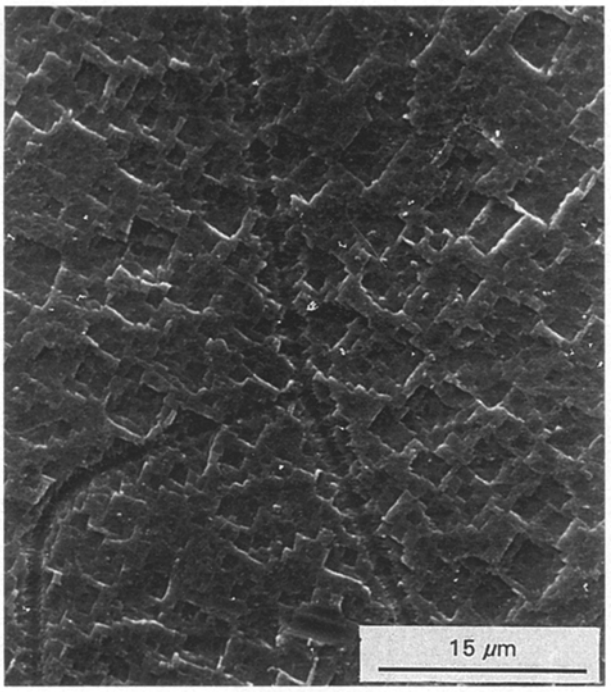

Figure 13 Scanning electron micrograph of orientation etch pits of the transverse cross-section of the wire. The control temperature was 1117 °C and the casting speed 120 mm min^{-1}.

will exhibit a triangular shape, while on a {0 0 1} plane, they will appear as square. Fig. 13 shows an example of orientation etch pits observed on the transverse cross-section of an OCC wire produced with a casting speed of 120 mm min^{-1}. The etchant was a nitric acid solution [12]. Well-developed boundaries were observed after etching. The square etch pit indicates that the preferred growth orientation perpendicular to the exposed plane of the crystal is in a ⟨0 0 1⟩ direction. Furthermore, it shows the aspect of misorientations between grains. By comparing the orientation of etch pits on both sides of the grains in Fig. 13, it is clear that the orientations of squares in the grains are almost identical, indicating that the misorientation between these grains is small, hence these boundaries are subgrain boundaries.

Because appropriate etchants must be used to produce etch pits on each specific plane [12], an attempt to observe etch pits for every specimen of unknown orientation is impractical. Thus, the crystal orientations were determined by using the electron channelling pattern (ECP) in an SEM. A series of specimens, sequentially produced with different casting speeds between 20 and 120 mm min^{-1}, were examined. The casting speed was increased intermittently from 20 mm min^{-1} to 120 mm min^{-1}, keeping the control temperature at 1117 °C and the mould–cooler distance at 33 mm. The length of the cast wires was approximately 1 m under each casting condition. The specimens were mechanically and electro-chemically polished prior to the channelling pattern analysis. The polishing conditions were 12 V and 2 A cm^{-2} and the electrolyte was a phosphoric acid solution (H_3PO_4:H_2O = 1:9). Typical examples of ECPs containing the major poles and bands are displayed in Fig. 14. The crystal orientations were determined by indexing these patterns (bands and poles) with reference channelling maps and an indexing guide for copper [13]. The results are plotted on a schematic channelling map shown in Fig. 15.

The growth orientations in the casting direction changed from ⟨0 1 1⟩ at a casting speed of 20 mm min^{-1} to ⟨0 0 1⟩ at a casting speed of 120 mm min^{-1}, implying that the casting speed has some influence on the preferred growth orientation of the crystal.

Yamamoto and Watanabe [10, 11] reported a preferred growth orientation in tin and zinc single crystals at fast growth rates and random orientation at slow growth rates. In order to determine if there is a correlation between the orientation and the casting speed for copper crystals, the other specimens produced with different casting conditions were examined. The results are shown in Fig. 16. Although, the growth orientation of the cast products cannot be predetermined by the casting speed, the results suggest that there is some influence on the orientation at higher casting speeds (~ 120 mm min^{-1}) where the predominant orientation was in the ⟨0 0 1⟩ direction. At lower casting speeds there did not appear to be an effect. It is interesting to note that the ⟨1 1 1⟩ direction did not appear among the samples examined.

Rosenberg and Tiller [14] reported that the preferred direction of growth was due to an impurity effect which changes the mode of solidification. They found that the growth orientation of an ingot made from zone-refined lead changed from the preferred orientation of ⟨1 1 1⟩ to random and then to a preferred orientation of ⟨0 0 1⟩ as the solidification interface structure changed from platelet to cellular by small additions of 5×10^{-5} to 10^{-4} wt % Ag. The preferred orientation observed in copper crystals may well be attributed to an impurity segregation effect at the interface caused by faster casting speeds, which in turn, changes the structure of the solid–liquid interface. Young and Savage [15] reported that for OFHC copper (~ 99.99%) and 99.999% purity copper, the crystals had no preferred orientation. However, in their work, the crystal growth rates were only 2.5 and 5 cm h^{-1}.

3.4. Orientation of stray grains

From observations of surface texture and macrostructure (Figs 8 and 9), it was found that for casting speeds above 60 mm min^{-1}, there was a tendency to form stray grains. Fig. 17 shows scanning electron micrographs of the area near the boundary between the stray grain and the matrix grain. In this case, the orientations of the square pits are significantly different on either side of the boundary, indicating that the boundary is a large-angle grain boundary. Thus stray grains are formed by separate nucleation events. From scanning electron micrographs (Fig. 17), the angular rotation of the stray grains with respect to the matrix grain can be roughly estimated, although the tilt component of misorientation cannot be determined. Misorientations (grain rotation) are found to be approximately in the range of 28°–57°. These observations were further confirmed by electron channelling

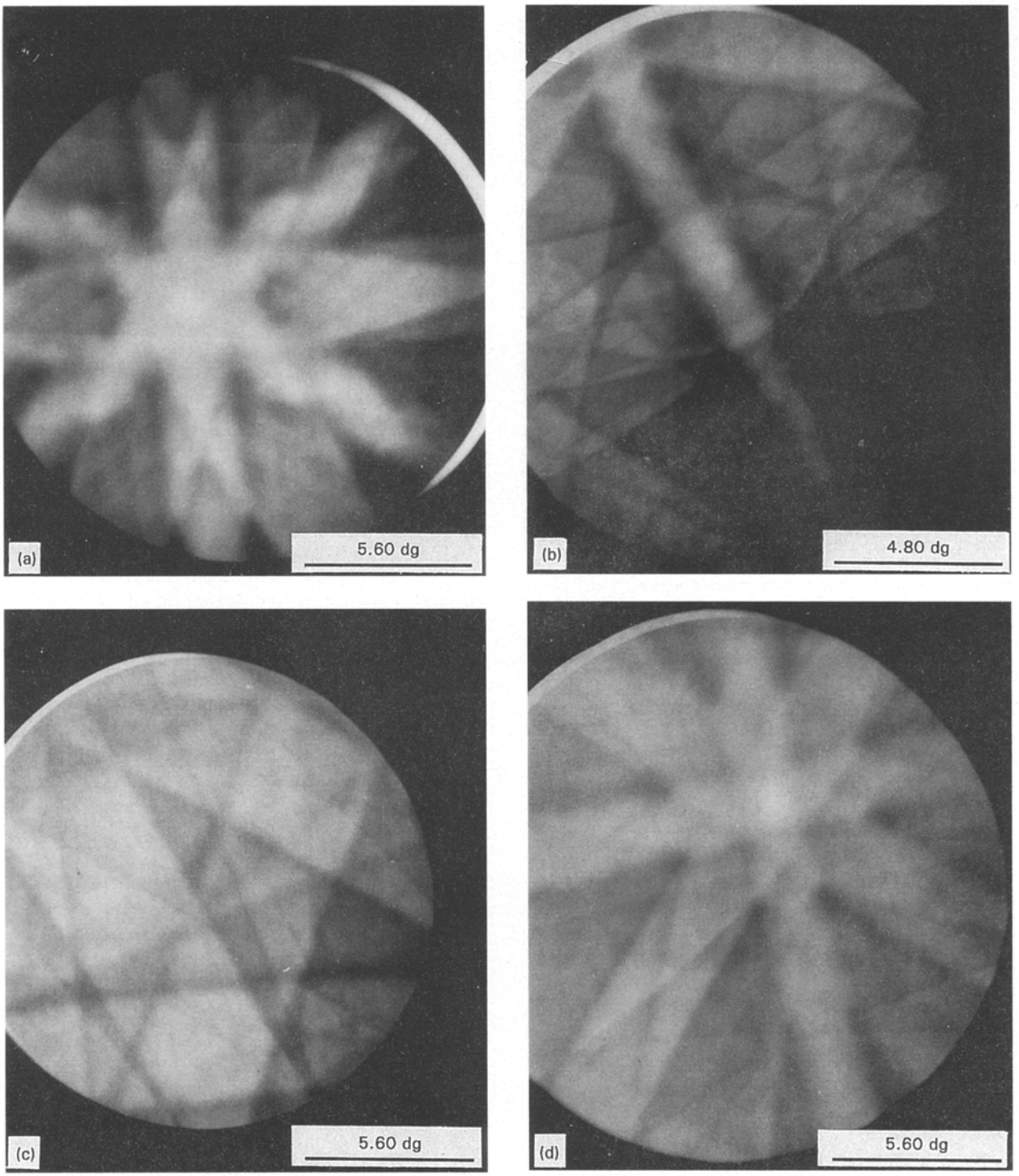

Figure 14 Electron channelling patterns taken from the transverse cross-section of the wires. Casting speeds: (a) 20, (b) 50, (c) 80, and (d) 120 mm min^{-1}.

pattern (ECP) analysis. Fig. 18 shows the electron channelling pattern from a sample area containing the stray grain and the matrix grain. In this case, the ECP was partly displaced by another pattern, due to a back-scattering signal coming from two separate grains. The ECP in Fig. 18 contains two separate $\langle 0\,0\,1 \rangle$ poles, indicating that the directions of both grains in the casting axis are in the vicinity of the $\langle 0\,0\,1 \rangle$ direction. As expected from the etch pit orientations, the major bands from one grain were found to be significantly rotated with respect to the direction of the bands from the other grain. The results show that the major orientation difference between the stray grain and the matrix grain is rotation about the casting direction.

3.5. Quality of single crystals

As previously shown in Fig. 11, numerous grains developed as the casting speed increased. In order to obtain a better understanding of the OCC copper materials, further ECP analysis was carried out on some of the samples produced with casting speeds between 20 and 120 mm min^{-1}. The ECP in an SEM can be used not only for the determination of crystal orientation but also for a rapid visual survey of the

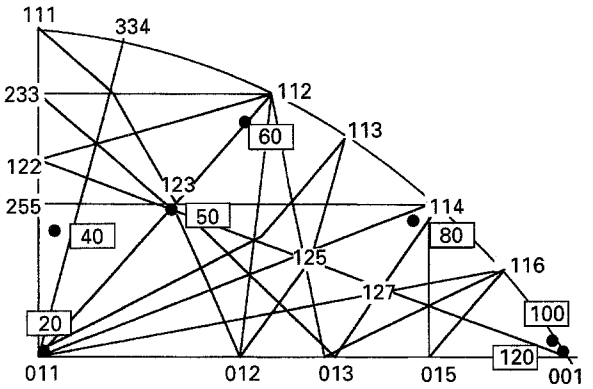

Figure 15 Growth orientations along the casting axis. The boxed numbers are the casting speeds (mm min^{-1}).

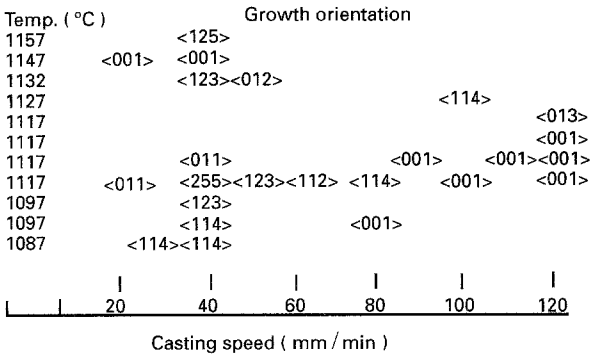

Figure 16 Crystal orientation of the specimens in the casting direction versus casting speed. Temp. (°C) is the control temperature.

perfection of a large single crystal [13]. From the channelling contrast on the CRT screen in an SEM, the presence of a boundary and a slight change in lattice orientation can be detected.

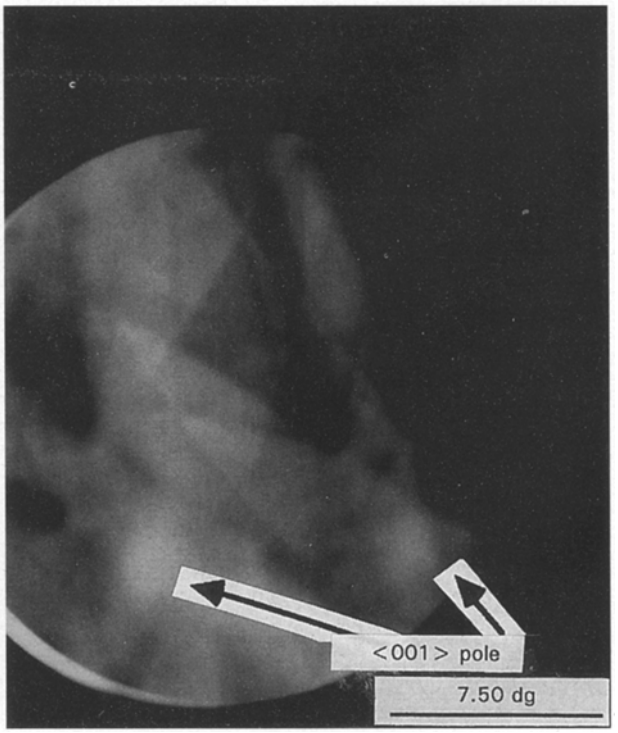

Figure 18 Electron channelling pattern containing two identical ⟨0 0 1⟩ poles. The casting speed was 100 mm min^{-1} and the control temperature 1117 °C.

In the case of the polycrystalline materials, when the scan area moves from point to point and crosses the grain boundary, the ECP will be completely or partly changed (Fig. 18). However, in the case of single crystals with no substructure, even if the scan area moves from one point to another, these displacements in the ECP should not occur, or should be very small if the scan area contains subgrains. In fact, the ECPs from

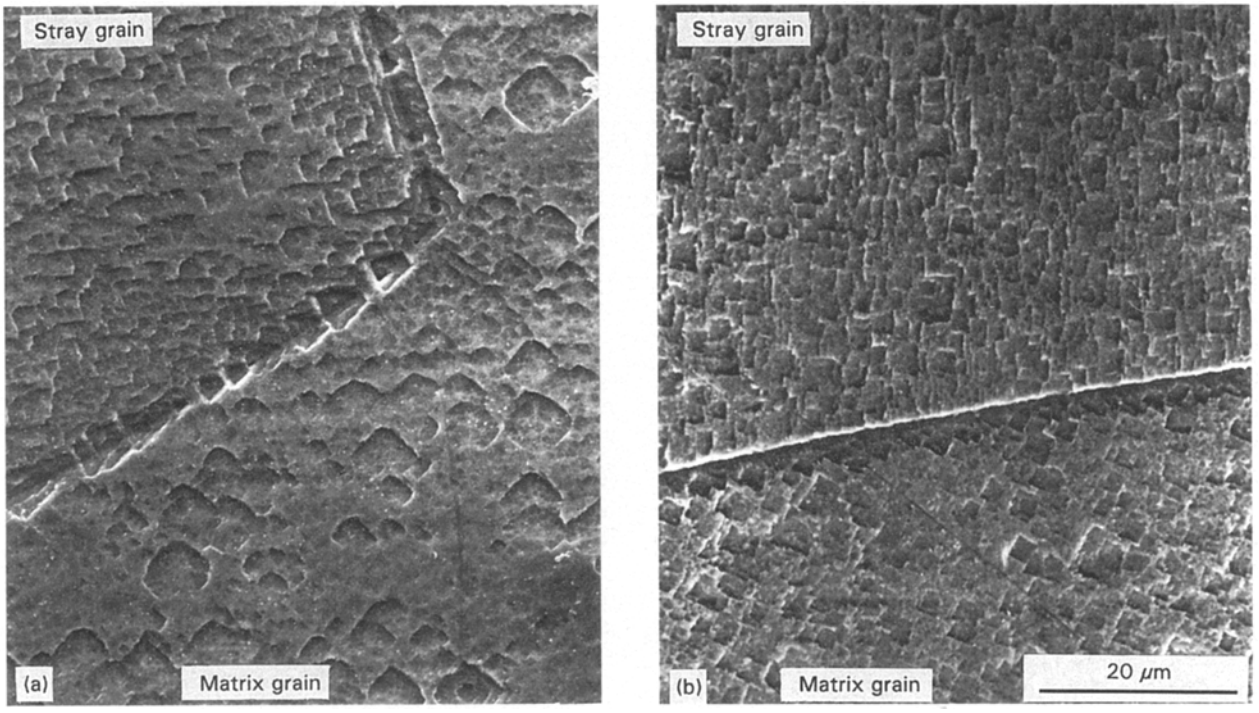

Figure 17 Orientation etch pits on the exposed surface of stray grain and matrix grain (transverse cross-section). The control temperature was 1117 °C and the casting speed was (a) 100 mm min^{-1} and (b) 120 mm min^{-1}.

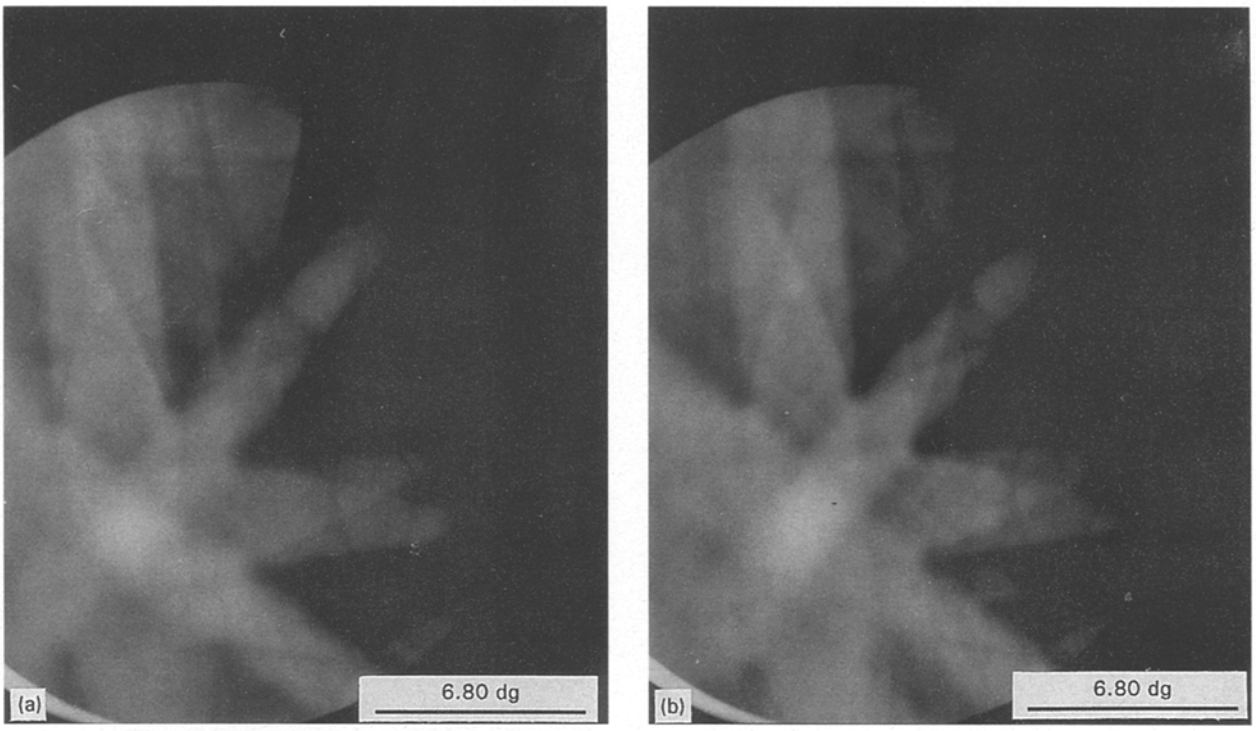

Figure 19 ECPs from the sample produced with a casting speed of 100 mm min^{-1}. ECP(b) was taken when a small shift was caused by moving the scan area by 0.5 mm from previous location, ECP(a).

samples produced with casting speeds of 20, 40 and 50 mm min^{-1} remained almost stationary on the screen. On the other hand, the ECPs from samples produced with casting speeds of 80, 100 and 120 mm min^{-1}, frequently exhibited small and abrupt movements on the screen when the scan area was moved horizontally over the specimen surface, indicating a slight change in the lattice orientation caused by the presence of subtexture within the material.

Fig. 19 shows ECPs from a sample cast at a speed of 100 mm min^{-1} during which the scan area was moved approximately 0.5 mm horizontally. This fluctuation indicates the presence of only a small misorientation in the sample. Indeed, the shift in the position of the pole (the degree of tilt) and the direction of the band (the degree of rotation) is very small. From Fig. 19, the misorientations were found to be less than one degree of tilt and four degrees of rotation.

Fig. 20 also shows small displacements (indicated by an arrow) in the ECP from a sample produced with a casting speed of 80 mm min^{-1} (compare with Fig. 14c). Again, the small displacements are evidence that misorientations are also small. From the results of these ECP analysis, it can be concluded that the aggregated grains observed in the OCC wire (e.g. Figs 8d and 11) are subgrains. The ECP analysis also reconfirms the results of the etch-pit observations.

For the specimen produced at a casting speed of 20 mm min^{-1}, the positions of the major pole and band in the ECPs remained constant, indicating the specimen is a single crystal with no major subgrains. These findings from ECPs further confirm the results of the external and internal texture observations, from which it can be concluded that a casting speed below 40–50 mm min^{-1} produces single crystals with no major subgrains. However, single crystals may still

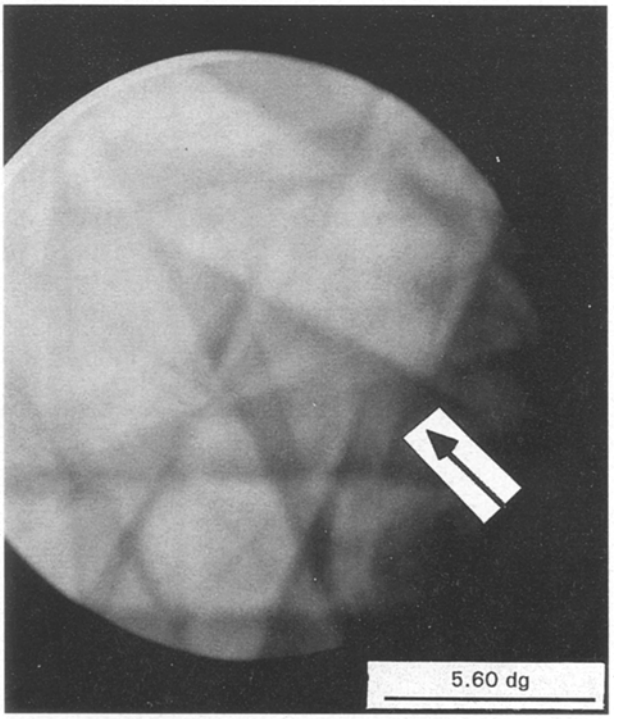

Figure 20 ECP from the sample produced with a casting speed of 80 mm min^{-1}.

contain cell-type subtextures caused by impurities or may contain small amounts of substructures, because ECPs taken at three different locations indicated a slight shift in the direction of the bands although the ECP did not appear to fluctuate during scanning, and furthermore the cast wire did not exhibit visible striations externally or internally.

The samples produced with casting speeds between 20 and 120 mm min^{-1} were examined by the Läue back-reflection X-ray technique to assess further the

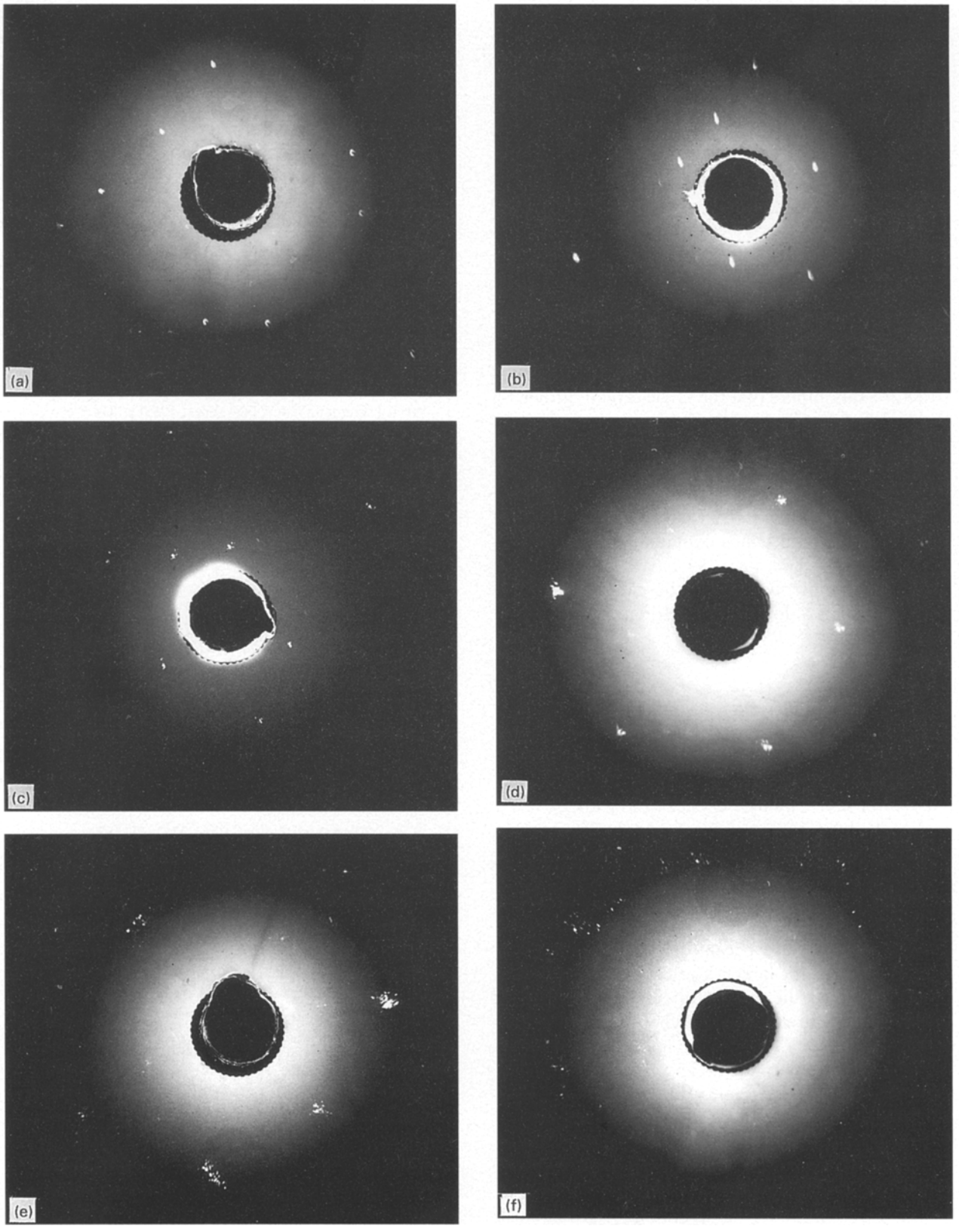

Figure 21 Back-reflection X-ray Läue pictures with casting speeds of (a) 20, (b) 40, (c) 50, (d) 60, (e) 100 and (f) 120 mm min^{-1}. The multiplicity of spots indicates the presence of subgrains.

quality of single crystals. Fig. 21 shows back-reflection X-ray pictures taken in the centre of the transverse cross-section of the specimens. The diameter of the X-ray beam at the surface of the specimen was 1 mm. The X-ray pattern shows that the multiplicity of spots changed as the casting speed increased. The multiple spots are more evident and diverse in the samples produced with faster casting speeds, while the pattern from the specimen produced with a casting speed of 20 mm min^{-1} shows that the spots are almost discrete, indicating the formation of a more perfect crystal.

The diversification of multiple spots indicates an increase in the number of subgrains as the casting speed increased. This implies that the degree of misorientation increased with an increase in casting speed. The widest spread in multiple spots was from

the specimen produced with a casting speed of 120 mm min^{-1}. This indicates the existence of a group of subgrains, the tilt angle of which differs from that of other groups of subgrains.

Wernick and Davis [16] produced copper single crystals by the Bridgman method and qualitatively evaluated them using Läue back-reflection X-ray work. In their study, the X-ray pattern showed asterism and multiplicity of spots. The X-ray patterns obtained from OCC specimens, produced with casting speeds of between 40 and 60 mm min^{-1} (Fig. 21b–d), are very similar to those reported by Wernick and Davis. Back-reflection X-ray pictures of OCC copper wire showing similar quality was also reported by Lew *et al.* [17]. Because the OCC wires produced at casting speeds of 50 and 60 mm min^{-1} contained visible substructure, this implies that the single crystals grown by Wernick and Davis using the Bridgman method must also have contained substructures. In fact, Lovell and Wernick [18], who studied dislocation etch pits for copper single crystals produced in the same equipment used by Wernick and Davis [16], showed that the single-crystal specimen contained lineage boundaries. Other workers [15, 19] have also shown the existence of numerous subgrain boundaries in copper single crystals produced by the Bridgman process.

4. Conclusion

This work was undertaken to obtain casting criteria for producing single-crystal copper wires, 4 mm in diameter, with the OCC process and then to evaluate the materials. It was found that at lower casting speeds (20–40 mm min^{-1}), single-crystal wires without visual surface texture were produced. At higher casting speeds (60–120 mm min^{-1}), there was a tendency to form stray grains and unidirectional subtexture. The casting speed has a significant influence on the development of this subtexture. With an increase in casting speed, the subtexture became clearer and the misorientations became larger. The preferred orientation of the crystal in the casting direction tended to be in a $\langle 001 \rangle$ direction at higher casting speeds ($\sim$ 120 mm min^{-1}). However, at lower casting speeds, the orientation was random. The growth orientation of stray crystals in the casting direction was found to be close to that of the matrix crystal and major misorientation was a rotation about the casting axis. Recrystallization occurred as wires left the mould when the cast surface was locally strained due to mould–strand friction. The quality of single crystals, 4 mm in diameter, produced with slower casting speeds by the OCC process, was comparable to those produced by the Bridgman method.

Acknowledgements

Financial support from the Japan Science and Technology Fund through the Natural Sciences and Engineering Research Council of Canada, ORTECH and Osaka Fuji Corporation, are gratefully acknowledged. The authors also thank P. Fortier and N. Wang, graduate students at the University of Toronto, for their help in electron channelling analysis.

References

1. A. J. GOSS, "The art and science of growing crystals" edited by J. J. Gilman (Wiley, New York, 1963) p. 314.
2. R. A. LAUDISE, "The growth of single crystals", Solid State Physical Electronics Series, edited by N. Holonyak Jr (Prentice-Hall, New Jersey, 1970) p. 141.
3. A. OHNO, *J. Metals* **38** (1) (1986) 14.
4. K. NAKANO, in "Proceedings of the Third International Conference on Solidification Processing" (The Institute of Metals, London, 1987) p. 413.
5. K. SAWADA, Y. NAKAI, H. SHIRAISHI, T. NAKANO, Y. MATSUSHITA and M. OJIMA, *Sumitomo Elect. Tech. Rev.* 27, January (1988) 140.
6. H. SODA, F. CHABCHOUB, S. A. ARGYROPOULOS and A. McLEAN, *Can. Metall. Q.* **31** (1992) 231.
7. H. SODA, G. MOTOYASU, F. CHABCHOUB, H. HU and A. McLEAN, *Cast Metals* **6** (1994) 225.
8. B. CHALMERS, "Principles of solidification" (Krieger, Malabar, FL, 1982) p. 307.
9. B. CHALMERS, *Can. J. Phys.* **31** (1953) 132.
10. M. YAMAMOTO and J. WATANABE, *Nippon Kinzoku Gakkai-Shi* **23** (1959) 675.
11. *Idem. ibid.* **23** (1959) 679.
12. F. W. YOUNG Jr, *J. Appl. Phys.* **32** (1961) 192.
13. D. C. JOY, D. E. NEWBURY and D. L. DAVIDSON, *ibid.* **53** (1982) R81.
14. A. ROSENBERG and W. A. TILLER, *Acta Metall.* **5** (1957) 565.
15. F. W. YOUNG Jr and J. R. SAVAGE, *J. Appl. Phys.* **35** (1964) 1917.
16. J. H. WERNICK and H. M. DAVIS, *ibid.* **29** (1956) 149.
17. S. S. LEU, W. H. WENG, G. C. LIU, S. F. CHANG and S. S. WU, in "Proceedings of the Annual Conference of the Chinese Society for Materials Science (Chinese Society for Materials Science, Chutung Hsinchu, Taiwan, 1992) p. 164.
18. L. C. LOVELL and J. H. WERNICK, *J. Appl. Phys.* **30** (1959) 590.
19. H. AKITA, D. S. SAMPAR and N. F. FIORE, *Metall. Trans.* **4** (1973) 1597.

Received 22 December 1994
and accepted 2 May 1995